RADIO CONTINUUM OBSERVATIONS OF *IRAS* SOURCES ASSOCIATED WITH DENSE CORES

L. F. RODRÍGUEZ[1,2] P. C. MYERS,[1] I. CRUZ-GONZÁLEZ,[2] AND S. TEREBEY[3]

ABSTRACT

Using the VLA, we searched at 6 cm for continuum emission associated with *IRAS* sources embedded in dense cores. We detected two new sources, 04016+2610 in L1489 and 19243+2350 in L778. The embedded sources have low luminosity ($L \lesssim 10\ L_\odot$). As in other similar sources, if the emission is free-free, the stellar radiation cannot account for the observed ionization rate. Two models that have been proposed to explain the radio continuum emission from low-luminosity stars are those of (partially) ionized winds and shock-induced ionization. For the two new sources and a previously reported one (HL Tau), the associated molecular outflow is of modest power. We show that under these conditions, these models, at least in their simplest versions, do not provide sufficient ionized gas. The nature of the radio continuum emission from low-luminosity young stars remains unexplained.

Subject headings: infrared: sources — radiation mechanisms — stars: formation — stars: radio radiation

I. INTRODUCTION

In the last few years, it has been established that dense cores in nearby molecular complexes are commonly the site of low-mass star formation. Beichman *et al.* (1986) found that 47 of 95 cores studied have an associated *IRAS* source. About half of these sources are visible T Tau stars, while the other half are optically invisible on Palomar Observatory Sky Atlas prints and presumably are even younger objects (Myers *et al.* 1987).

Sixteen cores with embedded *IRAS* sources were surveyed in the $J = 1 \rightarrow 0$ line of carbon monoxide for evidence of molecular outflows, with seven detections (Myers *et al.* 1988). This high detection rate also favors an early nature for the embedded objects. A similar conclusion was reached by Terebey, Vogel, and Myers (1989) in a combination of single-antenna and interferometer surveys for molecular outflows.

In this paper, we present the results of a radio continuum survey at 6 cm toward 12 dense cores. Our selection criteria were two: (1) the cores had at least one embedded *IRAS* source, and (2) one-half of the sample (B5, L1489, B35, L43, L778, L1172D) had associated CO outflow, while the other half (L1495, TMC 1A, L1527, L1152, L1082A, L1262) did not, at least to the limits of the Myers *et al.* (1988) survey. Radio continuum emission has been detected from several low-luminosity embedded young stars that appear to be powering molecular outflows. In a recent paper, Curiel *et al.* (1989) list several such continuum sources.

The radio continuum emission from low-mass young stars is a poorly understood phenomenon. If the radio emission is assumed to be thermal free-free radiation from a small H II region, the photoionizing rates required are those of an early B type star (Torrelles *et al.* 1985). But an early B star is orders of magnitude more luminous than the embedded objects surveyed and detected here. A nonthermal mechanism is also questionable because the few sources studied in detail (Snell and Bally 1986; Rodríguez *et al.* 1989) do not show obvious time variability, they have flat or rising spectra, and they are sometimes extended. Our study increases the number of

molecular outflows with known continuum emission. But because of the low luminosity of the sources reported here, neither photoionization nor shock ionization from stellar winds can easily explain the observations.

II. OBSERVATIONS

The observations were made in 1987 March 19 and 29 and 1987 June 4 with the Very Large Array of the National Radio Astronomy Observatory[4] in the D configuration. The March 19 and 29 observations were dedicated to a 6 cm survey of the 12 dense cores. We used 3C 286 as an absolute amplitude calibrator. The data were edited and calibrated using the standard VLA procedures. Maps of $12\farcm8 \times 12\farcm8$ and natural weighting were made and cleaned using the AIPS task MX to search for sources within the primary beam. The sources, phase centers, phase calibrators, beam sizes, and rms noises achieved in the maps are given in Table 1. The rms noise for the L1172A field is much higher than average because of the presence of a strong background source.

We detected a total of 41 radio sources in the fields observed. The positions and peak fluxes of the sources are given in Table 2. None of the sources detected exhibits significant extended structure with respect to our angular resolution of $\sim 15''$–$20''$. For our typical detection threshold (0.35 mJy), we expect (see the Appendix) on the average 3.1 background sources per field and a total of about 37 sources in all fields. Since 41 sources were detected, we conclude that most are background objects. It appears, however, that some are associated with the cores (see § IIIa).

III. DISCUSSION

a) Associations between Radio Sources and IRAS Point Sources

In the 12 fields mapped by us, there are a total of 30 *IRAS* point sources. The resulting density of *IRAS* sources is then 0.015 sources per square arcmin. We found three radio sources within the error ellipsoids of the *IRAS* sources (see Table 3). The associations are most probably real, based on the following argument. The probability of finding an *IRAS* source in a

[1] Harvard-Smithsonian Center for Astrophysics.
[2] Instituto de Astronomía, UNAM.
[3] Canadian Institute for Theoretical Astrophysics.

461

TABLE 1

DENSE CORES OBSERVED

SOURCE	NH$_3$ CORE REFERENCE	PHASE CENTER α(1950)	PHASE CENTER δ(1950)	PHASE CALIBRATOR	BEAM SIZE	rms NOISE (mJy)	MOLECULAR OUTFLOW?
B5	1	03^{h}44^{m}31^{s}8	+32°42'32"	0400+258	15".5 × 15".0	0.05	Y
L1489	2	04 01 40.6	+26 10 49	0400+258	15.8 × 14.6	0.05	Y
L1495	2	04 10 49.3	+28 03 57	0400+258	15.7 × 14.7	0.05	N
TMC 1A ...	3	04 36 31.2	+25 35 56	0400+258	15.8 × 14.9	0.05	N
L1527	3	04 36 49.3	+25 57 16	0400+258	15.7 × 15.3	0.06	N
B35	2	05 41 45.3	+09 07 40	0529+075	17.0 × 14.8	0.06	Y
L43	2	16 31 38.0	−15 40 50	1730−130	24.9 × 15.1	0.06	Y
L778	2	19 24 24.4	+23 52 24	1923+210	17.8 × 17.2	0.05	Y
L1152	2	20 35 19.4	+67 42 31	2021+614	21.2 × 18.9	0.05	N
L1082A	3	20 52 04.7	+60 03 14	2021+614	19.4 × 18.0	0.05	N
L1172D	2	21 01 44.2	+67 42 23	2229+695	16.0 × 15.2	0.20	Y
L1262	2	23 23 48.7	+74 01 08	2229+695	23.9 × 17.2	0.06	N[a]

REFERENCES.—(1) Benson 1983; (2) Myers and Benson 1983; (3) Benson and Myers 1989. The phase center is the position of the *IRAS* source associated with the NH$_3$ core.

[a] In L1262 no molecular outflow was detected in the CO survey of Myers *et al.* 1988 with 48" resolution. But Terebey, Vogel, and Myers 1989 found an outflow using 6" resolution, and Padman and Brown 1989 found an outflow using 20" resolution.

TABLE 2

SOURCES DETECTED AT 6 CENTIMETERS

SOURCE	POSITION[a] α(1950)	POSITION[a] δ(1950)	PEAK FLUX[b] (mJy)
B5 (1)	03^{h}44^{m}11^{s}0	+32°42'39"	2.3
(2)	03 44 21.1	+32 42 39	0.3
(3)	03 44 42.9	+32 42 49	2.1
L1489 (1)	04 01 40.4	+26 10 47	0.5
(2)	04 02 02.9	+26 15 05	1.5
L1495 (1)	04 10 49.1	+28 02 30	0.3
(2)	04 10 51.9	+28 01 32	0.9
(3)	04 10 54.6	+27 59 18	3.5
(4)	04 10 57.3	+27 59 12	3.6
(5)	04 11 07.3	+28 04 40	3.9
TMC 1A (1)	04 36 18.9	+25 39 49	0.7
(2)	04 36 28.5	+25 41 50	3.8
(3)	04 36 52.1	+25 37 14	2.1
L1527 (1)	04 36 45.2	+25 59 38	2.1
(2)	04 36 46.1	+25 50 05	14.6
(3)	04 36 55.6	+25 56 18	1.4
(4)	04 37 03.3	+25 52 05	1.4
(5)	04 37 19.6	+25 59 15	2.4
B35 (1)	05 41 20.8	+09 07 17	3.6
(2)	05 41 23.5	+09 06 44	3.3
(3)	05 41 38.0	+09 08 45	2.0
(4)	05 41 59.3	+09 02 42	1.5
(5)	05 42 04.2	+09 02 16	11.3
(6)	05 42 08.8	+09 05 12	1.3
L43 (1)	16 31 32.9	−15 38 48	0.5
(2)	16 31 50.6	−15 43 06	8.9
L778 (1)	19 23 56.5	+23 48 58	17.7
(2)	19 24 22.7	+23 50 48	1.0
(3)	19 24 23.0	+23 50 14	1.2
(4)	19 24 23.9	+23 49 09	8.3
L1152 (1)	20 34 34.7	+67 45 28	26.6
(2)	20 35 03.0	+67 41 36	3.5
L1082A (1)	20 51 40.9	+59 59 20	0.7
(2)	20 51 41.9	+60 04 13	3.6
(3)	20 52 29.0	+60 01 37	0.3
L1172D (1)	21 01 53.3	+67 43 15	2.4
(2)	21 01 54.7	+67 41 14	1.0
(3)	21 02 04.8	+67 46 24	183.0
L1262 (1)	23 22 40.0	+74 01 09	0.5
(2)	23 22 45.8	+74 04 02	0.5
(3)	23 24 25.5	+74 03 59	0.4

[a] Positional errors are ~2".
[b] Corrected for primary beam response.

40" × 40" solid angle is ~0.007. Since we detected 41 radio sources, the expected number of chance *IRAS*-radio associations (defined as closer than 20") for all fields observed is only 0.27. We then conclude that all three associations are most probably significant.

b) Comments on Individual Sources

L1489(1), the radio source associated with IRAS 04016+2610, was reobserved at 6 and 2 cm during 1987 June 4. The 6 cm flux coincided (within the observational error of 20%) with the determination made in 1987 March. The 2 cm flux was 0.7 ± 0.1 mJy, giving a spectral index of 0.3 ± 0.2. Maps of the source at 6 and 2 cm are shown in Figure 1. The source appears unresolved, with $\theta_s \lesssim 3"$. The radio position (see Table 1) coincides very closely with the *IRAS* position as well as with the refined infrared position of Myers *et al.* (1987).

L1495 (5) is associated with *IRAS* 04111+2804, which appears as associated with the T Tau star FM Tau in the *IRAS* Point Source Catalog. However, the position of FM Tau is $\alpha(1950) = 04^h11^m07^s9$, $\delta(1950) = 28°05'18"$ (Herbig and Rao 1972), significantly displaced from both the radio and *IRAS* sources. As first noted by Rucinski (1985), an object projected more closely to IRAS 04111+2804 is HD 283447, a visible K type star with weaker chromospheric emission than that of typical T Tauri stars (Kutner, Rydgren, and Vrba 1986). The position of HD 283447 ($\alpha = 4^h11^m07^s28$; $\delta = +28°04'40".5$; epoch = 1950.0). coincides within 0".5 with that of the radio source L1495(5). This radio source was first detected by Kutner, Rydgren, and Vrba (1986), who showed that it is compact (<0".3) and that the radio and optical positions coincide within 0".1. The 6 cm flux measured by these authors in 1983 August (3.8 mJy) coincides very well with our 1987 March determination (3.9 mJy). Since this radio source is associated with a visible, apparently more evolved star, we will not consider it as associated with an embedded object.

L778(2) is associated with IRAS 19243+2350. Myers *et al.* (1988) suggested that IRAS 19243+2352, at ~1.2' to the north of IRAS 19243+2350, is the exciting source of the complex molecular outflow in the region. However, IRAS 19243+2350 also appears as a viable candidate since (1) it has associated radio continuum emission, a relatively common situation in exciting stars of molecular outflows, (2) it appears somewhat

TABLE 3
ASSOCIATIONS BETWEEN RADIO SOURCES AND *IRAS* SOURCES

RADIO SOURCE	*IRAS* SOURCE	SEPARATION	P.A. OF SEPARATION	*IRAS* ERROR ELLIPSOID		
				Major Axis	Minor Axis	P.A.
L1489 (1)......	04016+2610	0″	...	28″	16″	84°
L1495 (5)......	04111+2804	9	96°	100	18	78
L778 (2)......	19243+2350	18	244	52	24	71

better centered in the complex outflow pattern than IRAS 19243 + 2352 (see Fig. 4a of Myers *et al.* 1988), and (3) it has slightly higher 100 μm flux than IRAS 19243 + 2352.

c) The Nature of the Radio Continuum Emission

We can summarize our observational results as follows. We observed 12 dense cores with embedded *IRAS* sources. Two new radio continuum sources were detected in association with embedded *IRAS* sources. Both cases are also outflow sources. This result suggests a relation between the presence of outflow and that of radio continuum emission. Indeed, in the shock-induced ionization scenario first proposed by Torrelles *et al.* (1985), both phenomena have a common origin. A powerful stellar wind is shocked and deflected by dense circumstellar structures. A modest ionization, similar to that produced by an early B type star, can be created by the shock. The now collimated wind accelerates more tenuous and extended gas, producing a molecular outflow. This model has also been discussed by Pravdo *et al.* (1985), Bohigas *et al.* (1985), Rodríguez *et al.* (1986), Evans *et al.* (1987), Curriel, Cantó, and Rodríguez (1987), and Curiel *et al.* (1989). Unfortunately, even when our results are consistent with this relationship, they are based on a relatively small number of objects and do not have solid statistical significance. There are two additional problems. First, as noted by Myers *et al.* (1988), stars with outflows tend to have bolometric luminosities 3–4 times greater than those without outflows. Then, the radio continuum emission could be correlated with stellar luminosity and consequently detected only in association with the systematically more luminous sources with detectable outflows. Second, more recent, higher angular resolution studies (Terebey, Vogel, and Myers 1989; Padman and Brown 1989) have detected outflows in some of the sources originally classified as nonoutflow objects.

In an attempt to discuss the nature of the radio continuum emission found in asociation with low-luminosity outflow sources, we searched in the literature for sources that complied with the following criteria: (1) bolometric luminosity less than or equal to 100 $L_\odot$, (2) associated molecular outflow detected and mapped, and (3) have been searched for radio continuum emission. We found 21 sources, whose parameters are listed in Table 4. When possible, we took the momentum rate in the outflow, $\dot{P}$, from the compilation of Mozurkewich, Schwartz, and Smith (1986). Seven of these sources (33%) have associated radio continuum emission. Mundt, Brugel, and Bührke (1987) find a similar percentage of radio continuum detections (six out of 14, or 43%) for sources with optical jets. Of the four known sources with both molecular outflows and optical jets associated (HH 7–11, T Tau, L1551, and AS 353A), all but the last have radio continuum emission. Our sample of low-luminosity sources shows the well-known correlation between bolometric luminosity, L_*, and momentum rate in the outflow, $\dot{P}$, first discussed by Rodríguez *et al.* (1982). In Figure 2, we show this correlation. As it is also known, the momentum rate in the outflow greatly exceeds the photon momentum rate, L_*/c (see Fig. 2), ruling out a radiative origin for the outflow. In Figure 3, we show the radio flux normalized by the distance squared, $S_\nu d^2$, versus source luminosity. The solid line gives the expected value of $S_\nu d^2$, assuming optically thin free-free emission from ionized hydrogen with an electron temperature of 10^4 K. The Lyman-continuum fluxes adopted are those of a ZAMS star of the given luminosity (Thompson 1984). From this figure, it is evident that ionization by stellar photons fails by many orders of magnitude in explaining the observed radio emission in the seven detected low-luminosity sources.

We finally discuss the relation between $S_\nu d^2$ and $\dot{P}$. In Figure 4, we plot these two parameters against each other.
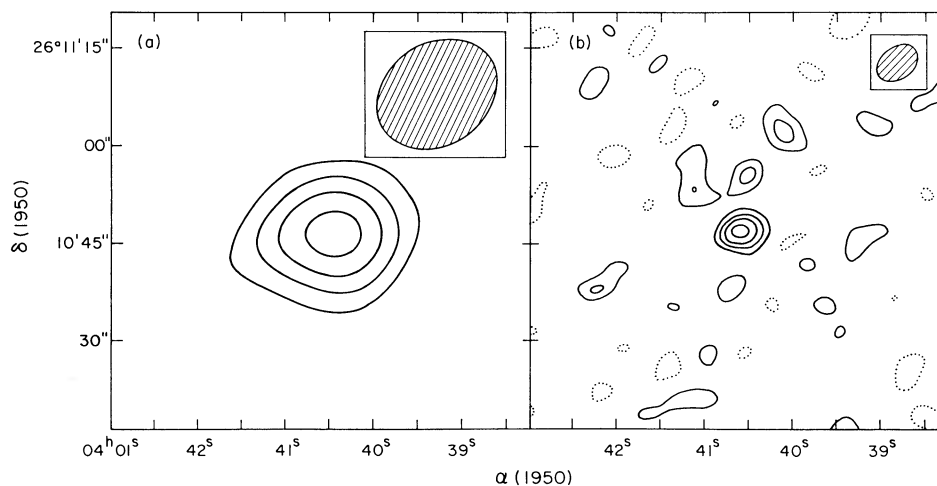

FIG. 1.—VLA maps of L1489 at 6 (a) and 2 cm (b). Contours are −0.3, 0.3, 0.5, 0.7, and 0.9 of the peak values of 0.51 and 0.74 mJy per beam.

TABLE 4

LOW-LUMINOSITY MOLECULAR OUTFLOW SOURCES WITH RADIO CONTINUUM OBSERVATIONS

Source	Distance (kpc)	Luminosity $(L_\odot)$	$\dot{P}$ $(M_\odot\,yr^{-1}\,km\,s^{-1})$	$S_{6\,cm}$ (mJy)	References
L1455	0.35	16	1.8 E−4	<0.5	1, 2
HH 7–11	0.35	58	1.1 E−3	0.8	3, 4
B5	0.35	5.8	6.7 E−5	<0.2	5, 6
L1489	0.14	2.9	2.0 E−7	0.5	6, 7
T Tau	0.14	17	4.1 E−5	5.8	8, 9
L1551	0.16	29	1.1 E−4	3.5	3, 9
HL Tau	0.16	44	1.4 E−6	0.3	8, 10
L1527	0.16	1	6.6 E−6	<0.3	2, 11
B35	0.46	14	1.1 E−5	<0.2	6, 7
HH 26 IR	0.5	40	6.8 E−4	<0.5	3, 4
L1598	0.9	49	1.6 E−4	<0.5	12
L1660	1.0	100	1.8 E−4	<0.5	12
IRAS 16293	0.16	27	1.6 E−3	2.9	13, 14
L43	0.6	2.5	5.0 E−7	<0.2	6, 7
L723	0.3	2.4	3.2 E−4	<0.4	1, 2
AS 353A	0.3	6.6	4.5 E−4	<0.2	3, 4, 15
L778	0.42	0.93	5.4 E−6	1.0	6, 7, 16
B335	0.4	7.6	2.0 E−5	<0.2	1, 2
PV Cep	0.5	80	2.3 E−4	<0.2	9, 17
L1172D	0.44	0.95	6.6 E−6	<0.6	6, 7
L1251	0.5	60	7.0 E−4	<0.5	12

REFERENCES.—(1) Goldsmith *et al.* 1984; (2) Schwartz *et al.* 1985; (3) Edwards and Snell 1984; (4) Snell and Bally 1986; (5) Goldsmith, Langer, and Wilson 1986; (6) this paper; (7) Myers *et al.* 1988; (8) Calvet, Cantó, and Rodríguez 1983; (9) Cohen, Bieging, and Schwartz 1982; (10) Brown, Mundt, and Drake 1985; (11) Frerking and Langer 1982; (12) Schwartz, Gee, and Huang 1988; (13) Wootten and Loren 1987; (14) Anglada, Estalella, and Rodríguez 1989; (15) Cohen and Bieging 1986. (16) Herbst *et al.* 1982; (17) Levreault 1984.

There are two simple models that can be used to account for the radio continuum sources in terms of thermal emission. One is that of an ionized, spherically symmetric wind. We assume that the $\dot{P}$ derived from the CO observations equals $\dot{M}v$ from the wind, where $\dot{M}$ is the mass-loss rate and v is the terminal velocity of the wind. We further assume that $v = 200$ km s^{-1} and that the electron temperature in the ionized wind is 10^4 K.

From Panagia and Felli (1975), we then derive

$$\left(\frac{S_\nu d^2}{mJy\,kpc^2}\right) = 1.1 \times 10^5 \left(\frac{\dot{P}}{M_\odot\,yr^{-1}\,km\,s^{-1}}\right)^{4/3},$$

where S_ν is the flux at 6 cm. The dashed line in Figure 4 shows the prediction of this model. The points with $\dot{P} \geq 10^{-5}$ $M_\odot$
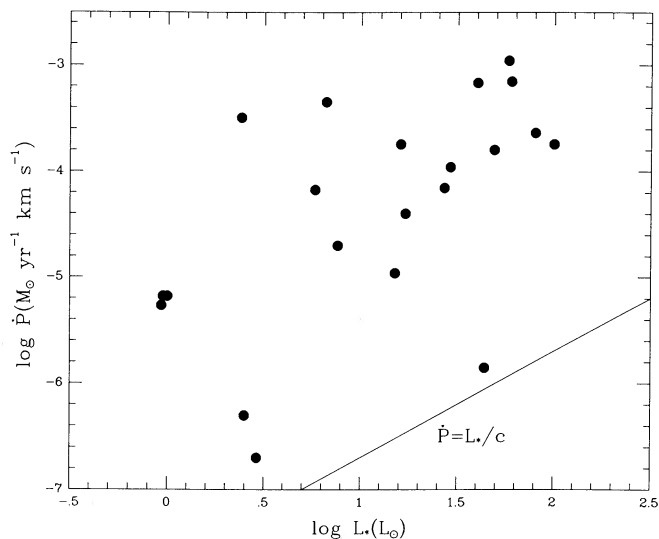

FIG. 2.—Momentum rate in the outflow vs. luminosity for the low-luminosity ($L_* < 100\,L_\odot$) sources. The solid line represents the momentum rate provided by radiation, which is insufficient by factors of 10–100.
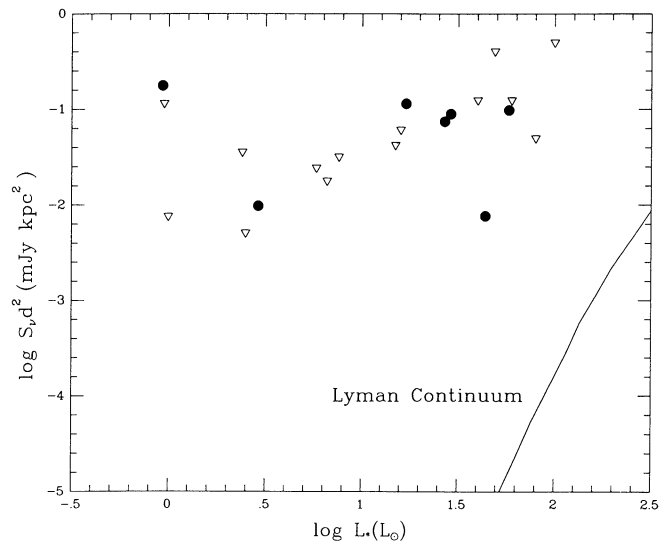

FIG. 3.—Flux density times distance squared vs. luminosity for the low-luminosity sources. The solid line represents the $S_\nu d^2$ values provided by Lyman-continuum radiation from a ZAMS star. The inverted triangles are upper limits.
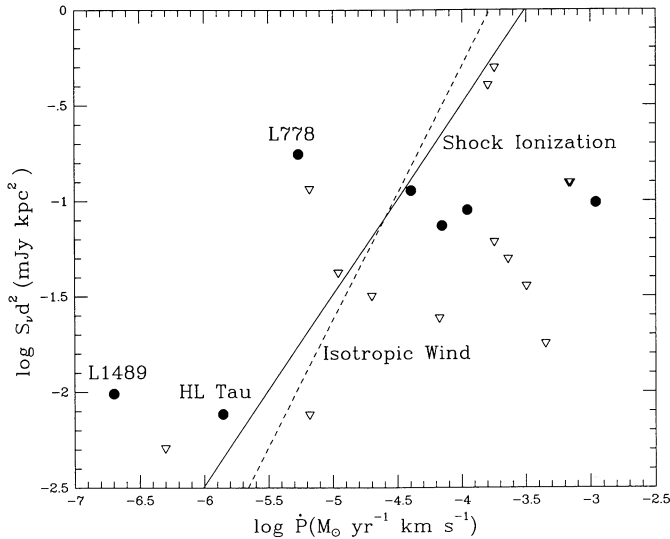
FIG. 4.—Flux density times distance squared vs. momentum rate in the outflow. The inverted triangles are upper limits. The solid line represents the prediction of a shock-ionization model, and the dashed line, that of a stellar wind model. Three sources (HL Tau, L1489, and L778) have $S_\nu d^2$ values in excess of the predictions of both models.

yr^{-1} km s^{-1} fall *below* the curve. This can be explained by proposing that the wind is only partially ionized, giving lower values of $S_\nu d^2$. However, the points with detected radio continuum and $\dot{P} < 10^{-5}$ $M_\odot$ yr^{-1} km s^{-1} (corresponding to HL Tau, L1489, and L778) fall *above* the model's prediction. A possible explanation for this problem is to propose that the stellar wind is collimated. As discussed by Schmidt-Burgk (1982) and Reynolds (1986), a collimated wind can produce, for a given value of $\dot{P}$, a much larger radio flux than an isotropic wind. Nevertheless, there is no satisfactory way of providing the observed ionization in the models of stellar winds of low-luminosity stars, since these winds are expected to be primarily neutral (Natta *et al.* 1988).

A similar problem occurs for the shock-ionization model. Making the same assumptions as for the stellar wind case, we get (Curiel *et al.* 1989):

$$\left(\frac{S_v d^2}{\text{mJy kpc}^2}\right) = 3.2 \times 10^3 \left(\frac{\dot{P}}{M_\odot \text{ yr}^{-1} \text{ km s}^{-1}}\right).$$

The prediction of this model is shown as a solid line in Figure 4. The points with $\dot{P} \geq 10^{-5}$ $M_\odot$ yr^{-1} km s^{-1} can be accounted for assuming that only a fraction of the wind is shocked against circumstellar material producing compact, detectable radio continuum emission. However, as in the case of the stellar wind model, the sources with detected radio continuum and $\dot{P} < 10^{-5}$ $M_\odot$ yr^{-1} km s^{-1} have a radio flux in excess of that predicted. An additional problem with the shock-ionization model is that it predicts optically thin radio continuum emission with the characteristic "flat" spectrum $S_\nu \propto \nu^{-0.1}$ (Curiel *et al.* 1989). At least for the cases of L1551 (Snell and Bally 1986), HH 1–2 VLA 1 (Rodríguez *et al.* 1989), and L1489 (this paper), where multifrequency observations are available, the spectrum seems to rise with frequency, $S_\nu \propto \nu^{0.3}$.

IV. ALTERNATIVE EXPLANATIONS

The three sources with modest $\dot{P}$ and detectable radio continuum emission (two of which are first reported here) appear to be in conflict with the predictions of the simplest version of the available models. However, given the present uncertainty in the nature of the phenomena involved, there are several possibilities to reconcile theory with observations. These possibilities are (1) the radio emission does not have a thermal nature; (2) the radio emission has a thermal nature but is not related to the outflow phenomenon; and (3) we are underestimating $\dot{P}$ (as a result, for example, of projection effects). In what follows we discuss these possibilities separately.

a) Nonthermal Radio Emission

The radio emission detected in association with low-luminosity stars that drive molecular outflows is relatively weak, and this has made difficult the accurate determination of its parameters. Within these limitations, to our knowledge none of the sources has negative spectral index, significant polarization, or confirmed time variability. Additionally, at least the source asociated with L1551 IRS 5 is extended (Rodriguez *et al.* 1986). These characteristics are suggestive of a thermal nature but, unfortunately, do not rule out a possible nonthermal origin. A major advance in the determination of the nature of the emisssion could be achieved with a thorough program of spectral index determination, high angular resolution mapping, and time monitoring of the known sources at the VLA.

b) Thermal Emission Unrelated to the Outflow Phenomenon

The first aspect of this possibility, is that, even when the radio continuum emission and the outflow are both the result of stellar wind activity, each phenomenon may be reflecting different epochs. The typical dimension of the outflows is ~ 0.1 pc. For the radio continuum sources we crudely adopt $\lesssim 0.01$ pc. If we assume that energy injection takes place in the form of a 200 km s^{-1} wind, the molecular outflows reflect an "average" of the stellar wind activity over the last 500 yr, while the radio continuum sources do the same but only over the last 50 yr or less. Since variability is not uncommon in pre–main-sequence stars, a rise in stellar activity over the last few decades could explain the presence of a radio continuum source even in weak outflow sources.

The second aspect of this possibility is that perhaps radio continuum emission is present in embedded sources regardless of the power of the outflows associated. This issue could be settled by surveying with the VLA a large sample of low-luminosity embedded sources with a wide range of $\dot{P}$ values.

c) Is $\dot{P}$ Underestimated?

The value of $\dot{P}$ from molecular observations is, as a matter of fact, rather uncertain. In particular, if the outflow axis is near perpendicular to the line of sight, the derived $\dot{P}$ will be a poor underestimate. A clear case of this situation is HH 1–2, with a powerful optical bipolar outflow traced by the proper motions of the HH objects (Herbig and Jones 1981), but no clear molecular outflow yet detected (Levreault 1988), which is the reason for its exclusion in our discussion even when the central exciting object is a radio continuum source (Pravdo *et al.* 1985). Of the three sources with radio fluxes above the model's predictions, HL Tau is only slightly above the predictions (see Fig. 4), and in the case of L778 some doubts may exist with respect to which *IRAS* source is powering the outflow. Then our best case for radio continuum excess is L1489. But for this source there is evidence from the optical that the outflow is more powerful than derived from the molecular observations alone,

since a large cometary cavity has been cleared by it (Heyer *et al.* 1989). It is then possible that in L1489 we may have a rather powerful outflow nearly perpendicular to the line of sight.

V. CONCLUSIONS

We searched, using the VLA, for 6 cm radio continuum emission toward 12 *IRAS* point sources embedded in dense cores. We detected two new sources, 04016+2610 in L1489 and 19243+2350 in L778. Both sources detected have associated molecular outflows, a result that is consistent with a possible relation between the presence of radio continuum emission and that of a molecular outflow.

In these and several other cases reported in the literature, the luminosity of the embedded source is too low to account for the radio continuum emission as coming from photoionized gas. We also consider the isotropic stellar wind and shock-ionization models to account for the radio emission. Some of the sources have continuum emission apparently in excess of the model's prediction, but the uncertainties in the determination of the radio continuum source and molecular outflow parameters preclude ruling out these models.

A significant advance in our understanding of the radio continuum emission from low luminosity embedded stars requires a considerable increase in the amount of available data.

APPENDIX

NUMBER OF BACKGROUND SOURCES EXPECTED AT 6 CENTIMETERS IN A VLA PRIMARY BEAM

We assume that the number of background sources per solid angle with flux equal or greater than S can be given by

$$N = aS^{-\alpha} ,$$

and that the primary beam response can be approximated by

$$P = P_0 \exp \left(-4 \ln 2 \, \frac{\theta^2}{\theta_A^2} \right) ,$$

where P_0 is the response in the center of the field, where $\theta = 0$, and θ_A is the half-power beamwidth. The detectable flux threshold in the field will go as

$$S = S_0 \exp \left(4 \ln 2 \, \frac{\theta^2}{\theta_A^2} \right) ,$$

where S_0 is the detectable flux threshold at the center of the field. Then the expected number of sources in all the field is

$$\langle N \rangle = \int_0^{\theta_{max}} N(\theta) \, 2\pi\theta \, d\theta ,$$

where

$$N(\theta) = a \left[S_0 \exp \left(4 \ln 2 \, \frac{\theta^2}{\theta_A^2} \right) \right]^{-\alpha} ,$$

and θ_{max} is an angular displacement large enough so as to have a very small primary beam response. We then make $\theta_{max} \to \infty$ and obtain

$$\langle N \rangle = aS_0^{-\alpha} \frac{\pi\theta_A^2}{\alpha 4 \ln 2} .$$

For 6 cm and $0.1 \text{ mJy} \leq S \leq 0.1 \text{ Jy}$, we derive from the data of Condon (1984) that

$$N = 40 \left(\frac{S}{\text{mJy}} \right)^{-0.75} (\text{deg})^{-2} .$$

For the VLA at 6 cm, $\theta_A = 9' = 0°15$, and we obtain

$$\langle N \rangle \simeq 1.4 \left(\frac{S_0}{\text{mJy}} \right)^{-0.75} .$$

This is then the number of sources expected in a map with a detectable threshold of S_0 and large enough to include all the solid angle where the primary beam has significant response. In our case, we made maps with a size of $\sim 1.4 \, \theta_A$. For a typical value of $S_0 = 0.35$ mJy, we expected ~ 3.1 sources per field.

REFERENCES

Anglada, G., Estalella, R., and Rodríguez, L. F. 1989, in preparation.
Beichman, C. A., *et al.* 1986, *Ap. J.*, **307**, 337.
Benson, P. J. 1983, Ph.D. thesis, Department of Physics, Massachusetts Institute of Technology.
Benson, P. J., and Myers, P. C. 1989, *Ap. J. Suppl.*, **71**, 89.
Bohigas, J., *et al.* 1985, *Rev. Mexicana Astr. Ap.*, **11**, 149.
Brown, A., Mundt, R., and Drake, S. A. 1985, in *Radio Stars* (Dordrecht: Reidel), p. 105.
Calvet, N., Cantó, J., and Rodríguez, L. F. 1983, *Ap. J.*, **268**, 739.
Cohen, M., and Bieging, J. H. 1986, *A.J.*, **92**, 1396.
Cohen, M., Bieging, J. H., and Schwartz, P. R. 1982, *Ap. J.*, **253**, 707.
Condon, J. J. 1984, *Ap. J.*, **287**, 461.
Curiel, S., Cantó, J., and Rodríguez, L. F. 1987, *Rev. Mexicana Astr. Ap.*, **14**, 595.
Curiel, S., Rodríguez, L. F., Cantó, J., Bohigas, J., Roth, M., and Torrelles, J. M. 1989, *Ap. Letters Comm.*, in press.
Edwards, S., and Snell, R.L. 1984, *Ap. J.*, **281**, 237.
Evans, N. J., Levreault, R. M., Beckwith, S., and Skrutskie, M. 1987, *Ap. J.*, **320**, 364.
Frerking, M. A., and Langer, W. D. 1982, *Ap. J.*, **256**, 523.
Goldsmith, P., Langer, W., and Wilson, R. 1986, *Ap. J. (Letters)*, **303**, L11.
Goldsmith, P. F., Snell, R. L., Hemeon-Heyer, M., and Langer, W. D. 1984, *Ap. J.*, **286**, 599.
Herbig, G. H., and Jones, B. F. 1981, *A.J.*, **80**, 1232.
Herbig, G. H., and Rao, K. N. 1972, *Ap. J.*, **174**, 401.
Herbst, W., Miller, D. P., Warner, J. W., and Herzog, A. 1982, *A.J.*, **87**, 98.
Heyer, M. H., Campbell, B. G., Ladd, E. F., and Myers, P. C. 1989, in preparation.
Kutner, M. L., Rydgren, A. E., and Vrba, F. J. 1986, *A.J.*, **92**, 895.
Levreault, R. M. 1984, *Ap. J.*, **277**, 634.
———. 1988, *Ap. J. Suppl.*, **67**, 283.

Mozurkewich, D., Schwartz, P. T., and Smith, H. A. 1986, *Ap. J.*, **311**, 371.
Mundt, R., Brugel, E. W., and Bührke, T. 1987, *Ap. J.*, **319**, 275.
Myers, P. C., and Benson, P. J. 1983, *Ap. J.*, **266**, 309.
Myers, P. C., Fuller, G. A., Mathieu, R. D., Beichman, C. A., Benson, P. J., Schild, R. E., and Emerson, J. P. 1987, *Ap. J.*, **319**, 340.
Myers, P. C., Heyer, M., Snell, R. L., and Goldsmith, P. F. 1988, *Ap. J.*, **324**, 907.
Natta, A., Giovanardi, C., Palla, F., and Evans, N. J. 1988, *Ap. J.*, **327**, 817.
Padman, R., and Brown, N. 1989, in preparation.
Panagia, N., and Felli, M. 1975, *Astr. Ap.*, **39**, 1.
Pravdo, S. H., Rodríguez, L. F., Curiel, S., Cantó, J., Torrelles, J. M., Becker, R. H., and Sellgren, K. 1985, *Ap. J. (Letters)*, **293**, L35.
Reynolds, S. P. 1986, *Ap. J.*, **304**, 713.
Rodríguez, L. F., Cantó, J., Torrelles, J. M., and Ho, P. T. P. 1986, *Ap. J. (Letters)*, **301**, L25.
Rodríguez, L. F., Carral, P., Ho, P. T. P., and Moran, J. M. 1982, *Ap. J.*, **260**, 635.
Rodríguez, L. F., Ho, P. T. P., Torrelles, J. M., Curiel, S., and Cantó, J. 1989, *Ap. J.*, submitted.
Rucinski, S. M. 1985, *A.J.*, **90**, 2321.
Schmidt-Burgk, J. 1982, *Astr. Ap.*, **108**, 169.
Schwartz, P. R., Frerking, M. A., and Smith, H. A. 1985, *Ap. J.*, **295**, 89.
Schwartz, P. R., Gee, G., and Huang, Y. L. 1988, *Ap. J.*, **327**, 350.
Snell, R. L., and Bally, J. 1986, *Ap. J.*, **303**, 683.
Terebey, S., Vogel, S. N., and Myers, P. C. 1989, *Ap. J.*, **340**, 472.
Thompson, R. I. 1984, *Ap. J.*, **283**, 165.
Torrelles, J. M., Ho, P. T. P., Rodríguez, L. F., and Cantó, J. 1985, *Ap. J.*, **288**, 595.
Wootten, A., and Loren, R. B. 1987, *Ap. J.*, **317**, 220.

I. Cruz-Gonzalez and L. F. Rodríguez: Instituto de Astronomía, UNAM, Apdo. Postal 70-264, 04510 México, D. F., México

P. C. Myers: Harvard-Smithsonian Center for Astrophysics, 60 Garden Street, Cambridge, MA   02138

S. Terebey: CITA, University of Toronto, McLennan Labs, 60 St. George Street, Toronto, Ontario, Canada M5S 1A1